

Lateral Resistance of Shallow Foundations



NZSEE 2001
Conference

K. J. McManus

Department of Civil Engineering, University of Canterbury.

N. R. R. Burdon

Holmes Consulting Group, Auckland.

ABSTRACT: Three shallow foundations each 4.25 m wide x 4.6 m long consisting of a 100 mm thick slab “on-grade” with two foundation beams 600 mm wide embedded 450 mm were constructed in coarse granular material. Each was tested by shoving back-and-forth by a powerful hydraulic actuator with several cycles of quasi-static lateral loading. These tests were supplemented with several, simpler interface sliding tests performed on 2 m wide x 3 m long concrete slabs constructed “on-grade” using one or two layers of polymer damp-proof membranes.

Lateral loading of the slab and beam foundations caused a wedge type of failure mechanism with significant passive soil pressures acting against the vertical faces of the foundation beams. The passive soil wedge developing against the trailing beam lifted one side of the structure vertically leaving hollow space beneath the floor slab. For the somewhat narrow structures tested, significant rotations of the structure occurred.

A simple method of analysis was developed and found to give good predictions for the experimental results while accounting for all of the main parameters. The analysis predicts that lateral load capacity is highly sensitive to the eccentricity (height above ground) of the applied lateral load.

1 INTRODUCTION

The resistance of shallow foundations to lateral loads is often relied upon to transmit the base shear forces from the ground to a building during an earthquake. Considering the importance of this link in the lateral load path it receives little attention in current design practice in New Zealand.

An assumption is commonly made, either explicitly or implicitly, that the combination of sliding friction along the base of the structure and passive earth pressure acting against embedded foundation elements will have ample capacity to resist the design base shear.

However, the actual mechanisms of lateral load resistance for shallow foundations are quite complex and poorly understood. Development of passive earth pressure requires significant plastic deformations within the soil mass and corresponding large movements of the structure. The required earth deformations may not be compatible with the structure’s geometry. Also, sliding friction may be limited by the use of polymer based damp proof membranes.

Three possible failure mechanisms are commonly identified for shallow foundation systems (e.g. Clough and Duncan, 1991) as shown in Figure 1: “Wedge Failure”, “Flow-Under Failure”, and “Tip-to-Top Failure”. The “Wedge Failure” is based on classical Rankine passive earth pressure theory, and shows that vertical movement of the structure may be necessary to develop full lateral earth pressure against the foundation beams. The “Wedge Failure” figure also shows the inherent incompatibility between the mechanisms of sliding friction and passive earth resistance with development of the failure wedges lifting the structure off its base.

The “Flow-Under Failure” would apply only to very soft soils such as soft clays. If the foundation beams are spaced closely then a “Tip-to-Tip” failure may occur with shearing of the soil beneath the foundation beams prior to development of a wedge failure mechanism.

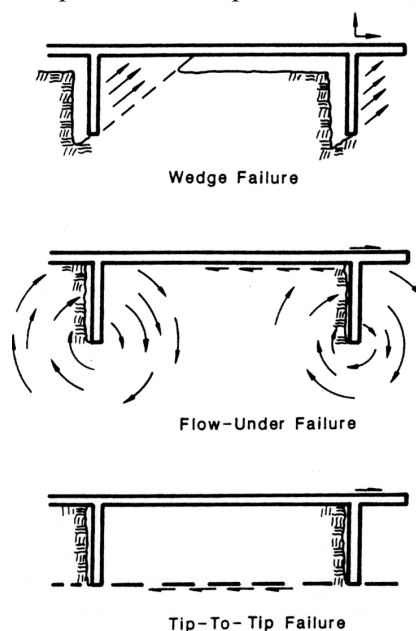


Figure 1. Failure mechanisms for shallow foundations with lateral loading. (Source: Clough and Duncan, 1991)

Murff and Miller (1977) developed equations for predicting the critical spacing of foundation beams necessary to generate a “Tip-to-Tip” failure mechanism. For the idealized foundation system shown in Figure 2, the lateral force developed for each foundation beam is given by:

$$F = 2k_a \sqrt{\frac{Qh}{k_a} + h} \quad (1)$$

in which k_a = weighted average shear strength of the soil, Q = vertical load, and h = depth of the foundation beams. The critical spacing of the foundation beams to generate a “Tip-to-Tip” failure then is given by:

$$\frac{q}{k_a} = 0.25 \left(\frac{k_h}{k_a} \right)^2 \frac{S}{h} - \frac{h}{S} \quad (2)$$

in which q = vertical load per unit area, k_h = horizontal shear strength of the soil, S = beam spacing.

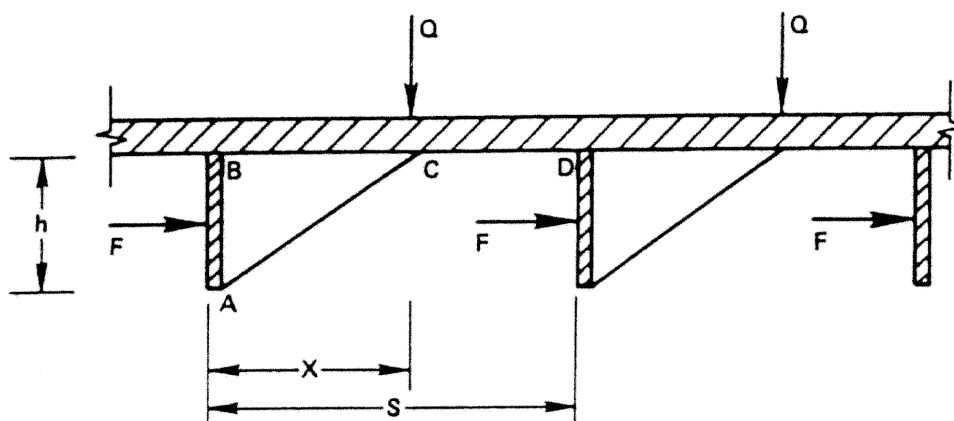


Figure 2. "Tip-to-Tip" failure mechanism. (Source: Murff and Miller, 1977).

The resulting relationship between vertical loading on the foundation and the critical foundation beam spacing is illustrated in Figure 3. The application of these results is limited in practice because the soil shear strengths k_a and k_h are only suitable for modeling the undrained soil condition, i.e. short term loading in silts and clays.

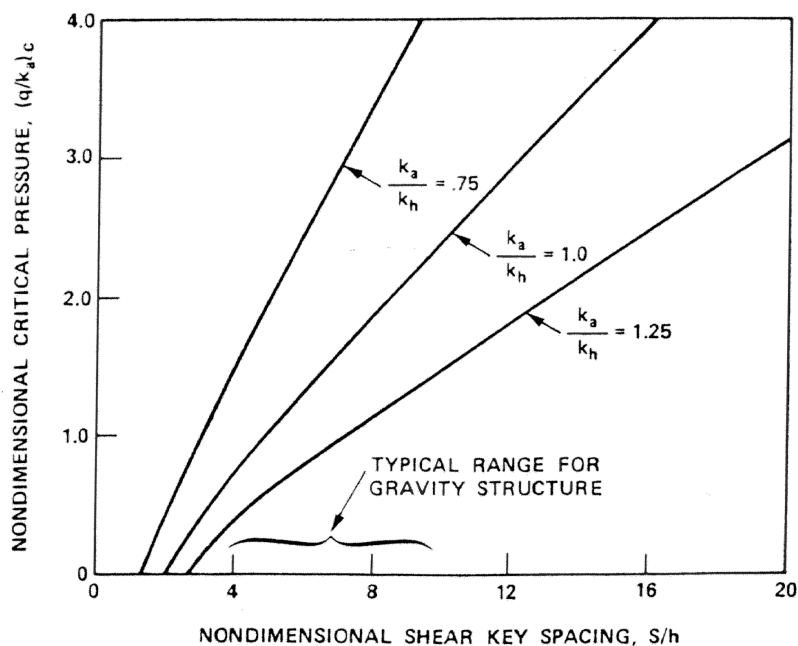


Figure 3. Critical foundation beam spacing for "Tip-to-Tip" failure. (Source: Murff and Miller, 1977).

Gadre and Dobry (1998) applied lateral loads to small-size square footings in a centrifuge at 30 g acceleration. The model dimensions of 38 mm x 38 mm x 28 mm deep scaled to prototype dimensions of 1.14 m x 1.14 m x 0.84 m deep. Significant degradation of lateral stiffness was observed at 25 mm displacement (prototype scale) with ultimate lateral resistance achieved at between 40 – 50 mm.

The objective in this present study was to gain better understanding of the mechanisms of lateral resistance of shallow foundations and to provide designers with both qualitative and quantitative guidance by field testing of full-scale but modest-size structures. Firstly, a series of simple sliding tests was performed to obtain data on the frictional characteristics of "slab-on-grade" foundations with polymer damp proof membranes (DPC). Then, more realistic structures combining both "slab-on-grade" and foundation beams were tested.

2 BASE SLIDING TESTS

The base sliding tests were intended to measure the sliding characteristics of typical “slab-on-grade” foundations. Concrete slabs 2 m wide x 3 m long x 135 mm thick were constructed without edge beams but otherwise using standard construction details and materials. One and two layers of DPC were used and some slabs were weighted with ballast. Each test slab was forced to slide back and forth parallel to its long axis while measurements of force and displacement were taken.

A diagram of the test setup is given in Figure 4. A wooden frame 3 m wide by 4 m long by 100 mm deep was constructed first. This was filled with pit-run granular material topped with a 25 mm thick sand blinding. The sand surface was leveled by screeding and then the DPC was rolled out and stapled to the wooden frame. The concrete slab then was constructed by pouring concrete into a steel form laying on top of the DPC. The concrete was cured for several days and then a hydraulic actuator was bolted to the slab and anchored to an adjacent large-size pile head. A 100 KN load cell was used to measure the force required to cause sliding while slab movement was monitored by a displacement transducer. Data was recorded electronically.

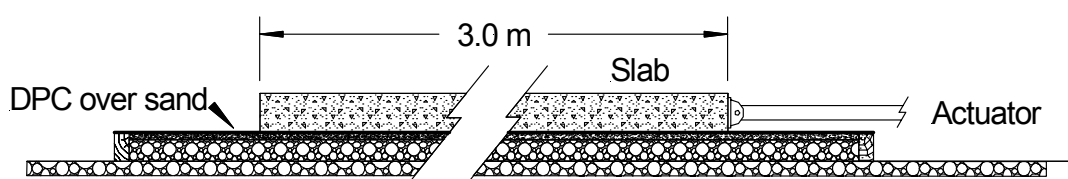


Figure 4. Section showing details of base sliding tests.

A simple test procedure was used as follows: each slab was pushed slowly, driven by a hand operated hydraulic pump, for 25 mm in one direction. Then the pump direction was reversed and the slab was dragged back to its starting position. Three or four cycles of load were applied in similar fashion until a steady load-displacement response was achieved. The results are summarised in Table 1.

Table 1. Base sliding friction for “slab-on-grade” foundations.

Foundation Type	Contact Pressure (KPa)	Peak Friction Angle (degrees)	Mean Friction Angle (degrees)
Single Layer DPC	3.0	23	21
	6.6	28	26
Two Layers DPC	3.1	12	10
	6.2	24	22

For some tests, the slab was ballasted by laying a previously tested slab on top supported on timbers laid at quarter points, effectively doubling the interface contact pressure. All tests were conducted on freshly made slabs.

For a single layer of DPC, there was a slight increase in friction with increased surcharge, probably caused by indentation of the sand grains into the soft material of the membrane. Some scuffing of the DPC was evident after testing.

Placing two layers of DPC resulted in halving of the interface friction angle for the single slab without ballasting. However, ballasting of the slab to 6.2 KPa caused the interface friction to increase significantly and to be nearly the same as for a single layer of DPC. This result is surprising and no explanation is immediately obvious. A small amount of “bulldozing” of sand occurred in front of each slab as it was pushed back and forth, more for the ballasted slabs than the unballasted slabs. However, the effect of such “bulldozing” should be the same whether one or two layers of DPC were used. Further testing of interface friction using increased weights of ballast are recommended to investigate this phenomenon.

3 COMBINATION SLAB AND BEAM EXPERIMENTS

Few foundations are ever made that consist only of “slab-on-grade” with no downturned foundation beams of some type. Most shallow foundations have foundation beams of some description together with floor slabs that are either suspended or built “on-grade”. Even when slabs are built “on-grade” they usually are structurally connected to the foundation beams, or should be. Isolated pad foundations supporting individual columns may also be part of a foundation design and sometimes these will not be inter-connected using beams. However, most foundations will have perimeter beams at least and it is beams that offer most potential for generating passive resistance to lateral movements. The effect of attached piles will be the subject of a further study.

A main objective of this study was to investigate the interaction between the passive resistance to lateral movement generated against vertical embedded surfaces such as beams and attached horizontal surfaces such as floor slabs. Therefore, a simplified structure consisting of two parallel foundation beams connected by a floor slab constructed “on-grade” was designed to incorporate the essential features of interest. Details of the structural design are given in Figure 5.

The structures were built as large as practicable given the limitations of available hydraulic actuators and field reaction points, the intention being to simulate behaviour at full-scale. Loads were applied by using a 500 KN MTS servo-hydraulic actuator under computer control. Measurements of load and horizontal displacement were collected electronically by using a Hewlett Packard HP34970 data acquisition system linked to a computer. Details of the loading system and test setup are shown in Figure 6.

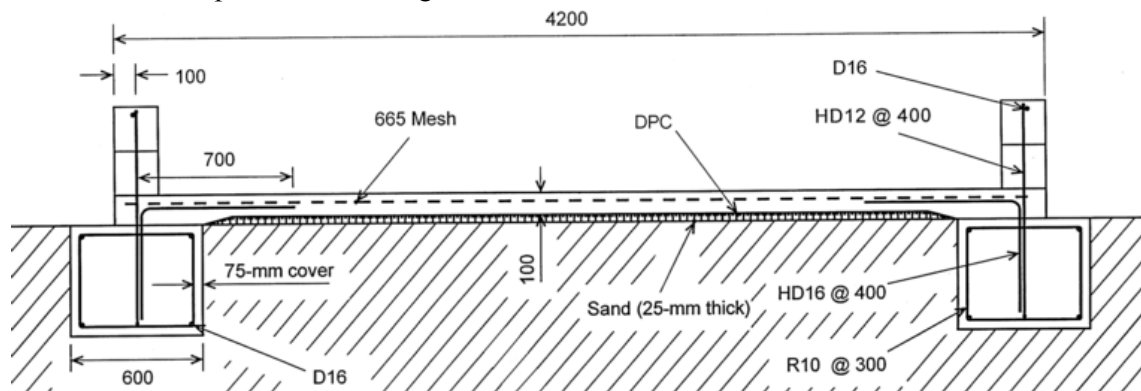


Figure 5. Section showing construction details of Test 3.

Three similar structures were built. The first acted somewhat as a shakedown test. Significant rotations of the structure occurred unexpectedly during loading and these caused the hydraulic loading system to apply undesirable moments which may have upset the results. For the second test, the loading system was re-designed to better accommodate rotation of the structure. The third test was ballasted by laying the first structure on top, effectively simulating a two storey structure.

The test procedure was essentially quasi-static. Each test proceeded as a series of shoves at a constant rate of displacement of 37.5 mm/min. At the end of each shove the test was stopped briefly so that observations of soil cracking, soil movements, structural rotation, and structural distress could be made. Then the direction of movement was reversed and the slab shoved to the opposite extreme of movement. For the first cycle of loading, the

shove was terminated once a steady state load had been reached. For subsequent cycles the structure was shoved to the full range of the actuator (+/- 76 mm).

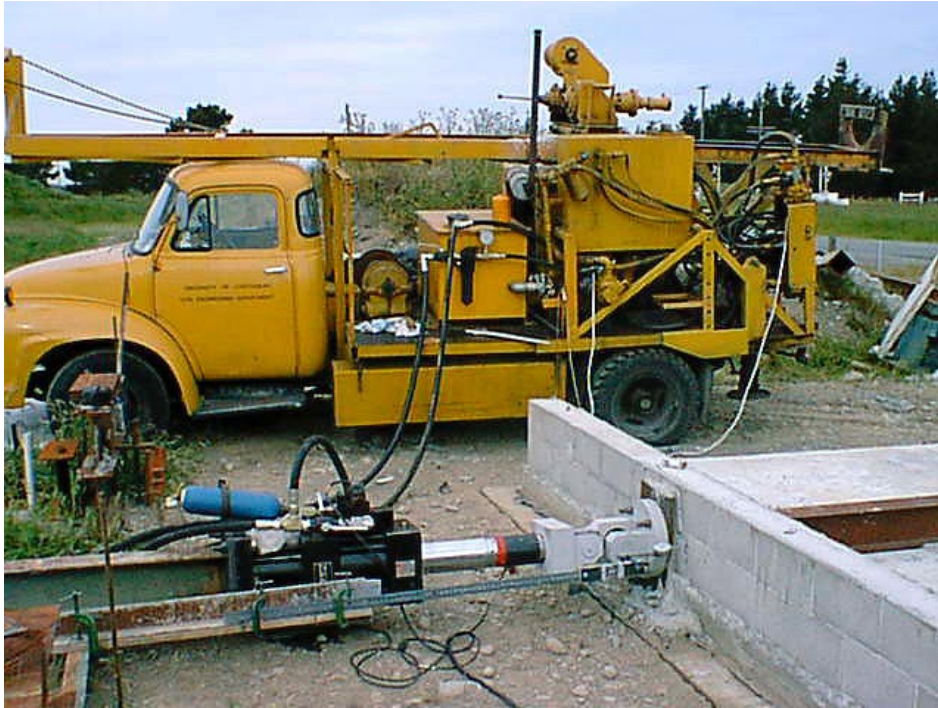


Figure 6. Load actuator setup for Test 2.

Load-displacement curves for Test 2 are shown in Figure 7 and for Test 3 in Figure 8. For Test 3, the ballasted “two-storey” structure, the 500 kN capacity of the actuator was barely adequate. The full lateral capacity of the structure appears to have been just mobilised in one direction and not quite in the other.

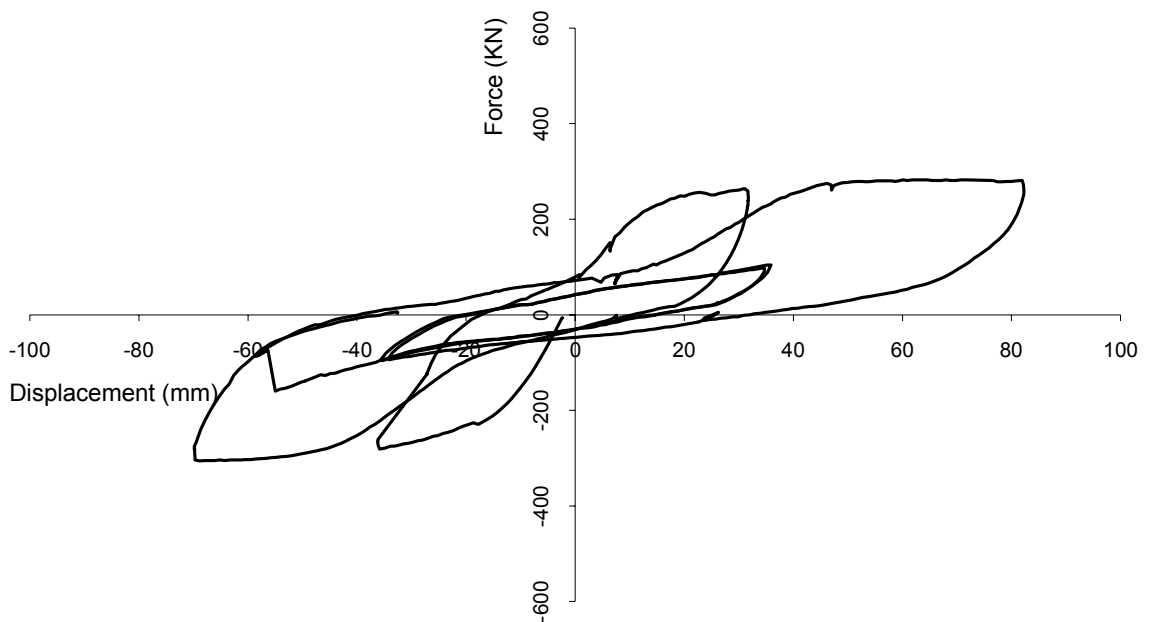


Figure 7. Load versus displacement for Test 2.

For Test 2, the HD16 bars tying the slab to the foundation beams were omitted and the slab failed in flexure. Also, the foundation beams were able to rotate somewhat independently of the slab, as seen in Figure 9. Rotation of the foundation beams should not have affected the mobilisation of soil passive pressure.

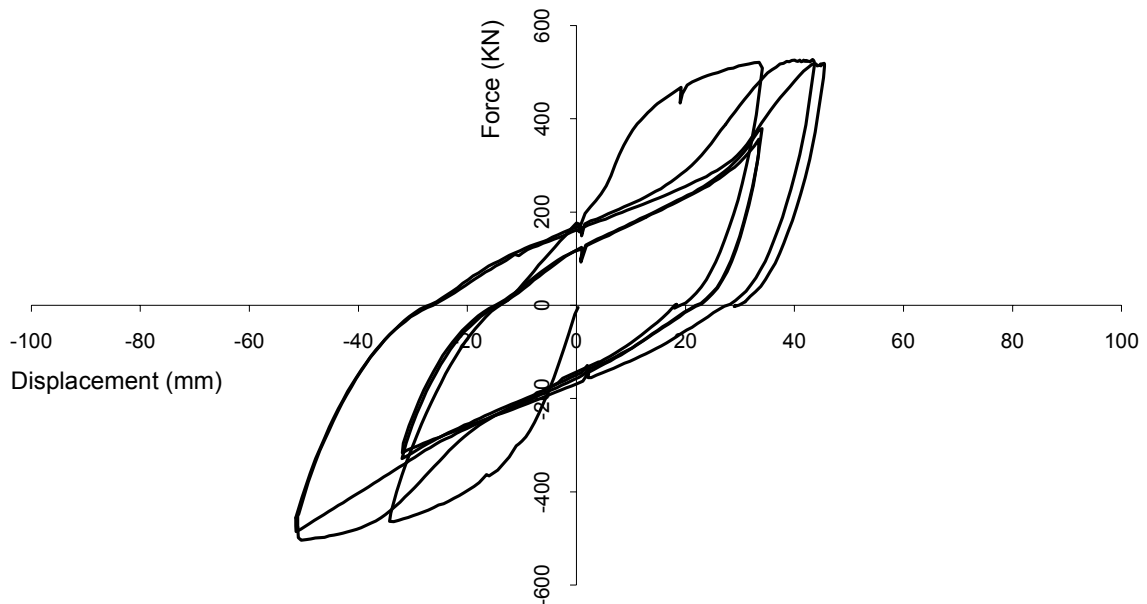


Figure 8. Load versus displacement for Test 3.

4 GENERAL OBSERVATIONS

The general failure mechanism for the structures under lateral loading was remarkably similar to the “Wedge Failure” cartoon of Figure 1. A clearly defined passive wedge developed under the slab in the direction of loading which “jacked” the structure up off the ground leaving a void under the slab. A single, significant difference from the cartoon is that, for the test structure, only one side was “jacked” off the ground because each foundation beam had slab attached to one side only, resulting in the motion indicated by the cartoon in Figure 10.



Figure 9. Rotation and uplift of foundation beam for Test 2. Arrow indicates location of the passive soil wedge.

A large gap opened up behind each foundation beam, as clearly seen in Figure 9, and as

predicted in the cartoon of Figure 1. This gap proved to be significant because when the direction of loading was reversed the gap had to close before passive soil resistance could be mobilised in the opposite direction, causing substantial “pinching” of the load-displacement curves.



Figure 10. Observed failure mechanism.

5 ANALYSIS OF RESULTS

From the observed general failure mechanism, the forces acting on the structure may be summarised as shown in Figure 11. R_1 and R_3 represent the passive earth pressure acting against the faces of the foundation beams. R_2 represents the additional lateral earth pressure from the force R_5 acting on the passive wedge as it lifts one side of the structure. The line of thrust of R_5 is assumed to act through the centre of the wedge. R_4 represents friction acting on the base of the foundation beam and F is the applied lateral load acting with eccentricity e .

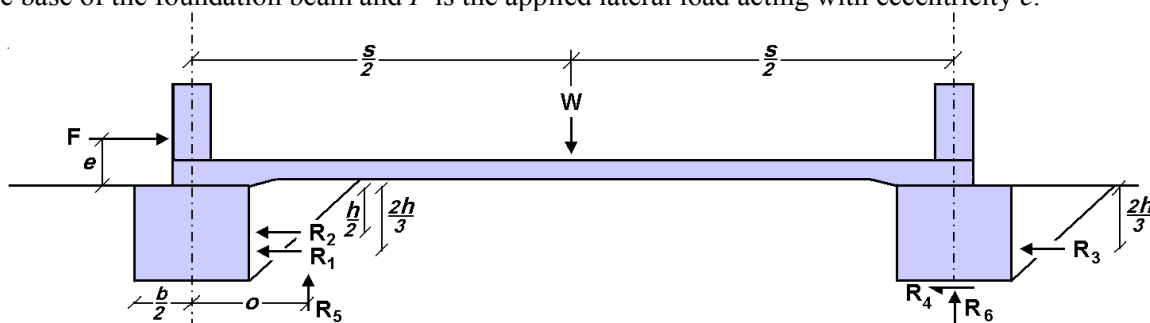


Figure 11. Forces acting on structure with lateral loading by force F .

Since the left hand beam is moving upwards with the passive soil wedge, there will be no friction acting on the vertical face of the beam and it may be treated as frictionless. Therefore, Rankine’s simple theory may be used to compute R_1 :

$$R_1 = 0.5K_p \gamma h^2 L \quad (3)$$

$$K_p = \frac{1 + \sin \phi_b}{1 - \sin \phi_b} \quad (4)$$

in which ϕ_b = the backfill material angle of internal friction, and L is the length of the foundation beam.

There will be friction between the right hand beam and the right hand passive wedge of soil. This friction tends to increase the passive resistance R_3 while simultaneously reducing R_6 and the resulting friction R_4 . The net effect on the total lateral resistance is probably negligible and so the simplifying assumption of a frictionless wall was applied to the computation of R_3 :

$$R_3 = R_1 \quad (5)$$

The remaining reaction forces are given by:

$$R_2 = R_5 K_p \quad (6)$$

$$R_4 = R_6 \tan \phi_g \quad (7)$$

$$W = R_5 + R_6 \quad (8)$$

in which ϕ_g is the interface friction angle between the base of the foundation beam and subgrade. The line of action of R_5 is given by:

$$o = \frac{h}{2} \tan(45^\circ + \frac{\phi_b}{2}) + \frac{b}{2} \quad (9)$$

An explicit expression for R_6 was obtained from consideration of rotational equilibrium of the structure, as follows:

$$R_6 = \frac{(R_1 + R_3)(1 + \frac{2h}{3e}) - W(\frac{o}{e} - \frac{s}{2e} - K_p(1 + \frac{h}{2e}))}{\frac{s}{e} - \tan \phi_g(1 + \frac{h}{e}) - \frac{o}{e} + K_p(1 + \frac{h}{2e})} \quad (10)$$

The lateral capacity then is given by:

$$F = R_1 + R_2 + R_3 + R_4 \quad (11)$$

Computations were made to predict the measured capacities for Tests 2 and 3 with the results summarised in Tables 2 and 3. Good agreement was obtained in both cases. The slight (6 – 10 percent) underestimate of capacity is probably because of a slight underestimate of the soil strength properties. The test soils were above the water table and were moist and might be expected to show some apparent cohesion. However, the soil strengths used in the computations are what a designer might reasonably estimate and the slight conservatism resulting is considered appropriate.

Table 2. Computed lateral capacity Test 2.

W	L	e	s	b	h	γ	ϕ_g	ϕ_b	F	Test 2*
(KN)	(m)	(m)	(m)	(m)	(m)	(KN/m ³)	(deg.)	(deg.)	(KN)	(KN)
118.1	4.25	0.125	4.0	0.6	0.45	17.2	40	35	263	292

* - average of both directions of loading

Table 3. Computed lateral capacity Test 3.

W	L	e	s	b	h	γ	ϕ_g	ϕ_b	F	Test 3*
(KN)	(m)	(m)	(m)	(m)	(m)	(KN/m ³)	(deg.)	(deg.)	(KN)	(KN)
233.4	4.25	0.125	4.0	0.6	0.45	17.2	40	35	482	515

* - average of both directions of loading

The computations are highly sensitive to changes in the ratio of load eccentricity (e) to width (s). Increasing load eccentricity causes transfer of structural weight from the left hand passive

wedge to the right hand beam (in Figure 11). This weight transfer significantly reduces the lateral resistance of the structure because weight applied to the left hand passive wedge is very effective, increasing the lateral earth pressure on the left hand beam by factor K_p (values typically 3 – 4).

With reversal of loading direction, as the structure moved back through its central position, lateral load resistance was observed to decrease to low values as the vertical faces of the foundation beams lost contact with the backfill material. For Test 2, by the third cycle of loading, lateral resistance had dropped to approximately 40 kN. The structure presumably was sliding on the DPC/sand interface with an equivalent friction angle of 19 degrees. For Test 3 the minimum lateral resistance at zero displacement was 114 kN, equivalent to a friction angle of 26 degrees. These friction values are close to the measured values for a slab sliding on a single layer of DPC suggesting that, between displacement extremes, the structure is simply sliding back-and-forth supported by the slab resting “on grade”.

6 CONCLUSIONS

Three shallow foundations each 4.25 m wide x 4.6 m long consisting of a 100 mm thick slab “on-grade” with two foundation beams 600 mm wide embedded 450 mm were constructed in coarse granular material. Each was tested by shoving back-and-forth by a powerful hydraulic actuator with several cycles of quasi-static lateral loading. These tests were supplemented with several, simpler interface sliding tests were performed on 2 m wide x 3 m long concrete slabs constructed “on-grade” using one or two layers of polymer damp-proof membranes.

Lateral loading of the slab and beam foundations caused a wedge type of failure mechanism with significant passive soil pressures acting against the vertical faces of the foundation beams. The passive soil wedge developing against the trailing beam lifted one side of the structure vertically leaving hollow space beneath the floor slab. For the somewhat narrow structures tested, significant rotations of the structure occurred.

A simple method of analysis was developed and found to give good predictions for the experimental results while accounting for all of the main parameters. The analysis predicts that lateral load capacity is highly sensitive to the eccentricity (height above ground) of the applied lateral load.

Full development of the lateral load resistance required 30 – 50 mm displacement. After being shoved to a displacement extreme in one direction, the structure was free to slide back in the opposite direction, with relatively low load resistance from base sliding friction only.

7 RECOMMENDATIONS FOR PRACTICE

Designers need to account for the significant vertical movements and redistribution of vertical loads caused by development of passive soil wedges adjacent to foundation beams with lateral loading. Also, knowledge of the overturning moment accompanying each pulse of lateral load is necessary to be able to predict the lateral load capacity of the foundation.

The method for computing lateral resistance of shallow foundations given by Equation 3 to 11 gave good predictions for the experimental results and could be extended to more complex foundations.

8 ACKNOWLEDGEMENTS

This study was funded by the EQC Research Foundation under project 99/423. John van Dyk constructed the experiments and assisted with the testing. The authors are grateful for his enthusiasm and “can do” spirit.

REFERENCES:

Clough, G.W., Duncan, J.M. (1991) “Earth Pressures”. In: Foundation Engineering Handbook

2nd Edition. Ed: Fang, H., Chapman & Hall, New York

Gadre, A., Dobry, R. (1998) "Lateral cyclic loading centrifuge tests on square embedded footing." *Journal Geotechnical and Geoenvironmental Engineering*. 124. 1128-1138

Murff, J.D. and Miller, T.W. (1977b), Stability of offshore gravity structure foundations by the upper-bound method, *Proceedings of the Offshore Technology Conference*, 3, pp. 147-154

9 RETURN TO INDEX

